
ADAPTIVE POD GALERKIN TECHNIQUE FOR RESERVOIR SIMULATION AND OPTIMIZATION

A PREPRINT

 **Dmitry Voloskov**

Skolkovo Institute of Science and Technology
3 Nobelya st., Moscow, Russia 121205
dmitry.voloskov@skoltech.ru

Dimitri Pissarenko

Skolkovo Institute of Science and Technology
3 Nobelya st., Moscow, Russia 121205
d.pissarenko@skoltech.ru
TOTAL S.A.
7 Lesnaya st., Moscow, Russia 124196

August 2020

ABSTRACT

In this work, a novel method with an adaptive functional basis for reduced order models (ROM) based on proper orthogonal decomposition (POD) is introduced. The method is intended to be applied in particular to hydrocarbon reservoir simulations, where a range of varying boundary conditions must be explored. The proposed method allows us to update the POD functional basis constructed for a specific problem setting in order to match varying boundary conditions, such as modified well locations and geometry, without the necessity to recalculate each time the whole set of basis functions. Such an adaptive technique allows us to significantly reduce the number of snapshots required to calculate the new basis, and hence reduce the computational cost of the simulations. The proposed method was applied to a two-dimensional immiscible displacement model, and simulations were performed using a high resolution model, a classical POD reduced model, and a reduced model whose POD basis was adapted to varying well location and geometry. Numerical simulations show that the proposed approach allows us to reduce the required number of model snapshots by a few orders of magnitude compared to a classical POD scheme, without noticeable loss of accuracy of calculated fluid production rates. Such an adaptive POD scheme can therefore provide a significant gain in computational efficiency for problems where multiple or iterative simulations with varying boundary conditions are required, such as optimization of well design or production optimization.

Keywords Reservoir Simulation · Reduced Order Model · Proper Orthogonal Decomposition · Production Optimization

1 Introduction

Fluid flow simulation in subsurface porous media is an essential process in virtually all reservoir engineering applications. Hydrodynamic reservoir models are typically based on a numerical solution of a system of nonlinear partial differential equations [1] that describe the evolution in time of pressure field and fluid flow. These equations are discretized using such numerical methods as finite volumes [2] or finite elements [3], and are solved using IMPES (implicit pressure, explicit saturation), sequential, or fully implicit schemes [4, 5, 6]. In order to accurately reflect structural and physical complexities of a hydrocarbon reservoir, the numerical model should typically contain millions of cells. Numerical simulations based on such models inevitably become a very challenging computational task. Another factor that additionally increases the computational complexity of reservoir models is the non-linearity of the governing equations. As a result, industry grade reservoir simulations are a very resource consuming task that usually requires the use of high performance computing hardware. The same reason justifies a significant effort by the reservoir simulation community aimed at improving the computational efficiency of the simulations either through parallelization or by algorithmic means. Regardless of such improvements, the computational cost and consequently

the duration of the simulation often become prohibitive for such classes of problems as reservoir optimization and uncertainty quantification: they typically require to perform thousands of runs of simulation scenarios.

In this paper, an applications of the Reduced Order Modeling (ROM) approach to reservoir simulation problems where a range of boundary conditions needs to be explored, is considered. A new variant of proper orthogonal decomposition (POD) method, that allows us to considerably decrease the amount of calculations for each particular set of boundary conditions, and hence to reduce the overall computational cost of the problem, is introduced. ROM methods and their applications to resource demanding simulations in various areas of science and engineering are actively explored in the recent years [7, 8, 9, 10]. A class of ROM methods frequently applied to large-scale simulation problems are based on POD. In these methods, POD is used in order to obtain a consistent representation of a model in a functional space whose dimension is lower than that of the original model. To that end, the model's state variables are projected onto a lower-dimensional POD domain, and Galerkin or least-squares Petrov-Galerkin projection is applied in order to obtain a reduced system of equations [11].

One of the main difficulties in the realization of efficient POD-based ROMs is related to handling the non-linearities of the model's equations. In iterative algorithms frequently used for solving non-linear systems of equations such as Newton method, calculations of the non-linear terms and the Jacobian estimation are required. To do so, one generally needs to project the approximated solution back to the original domain and calculate the nonlinear functional in the full-scale domain on every iteration of the algorithm. The cost of such full scale non-linear functional calculation and of the forth-and-back projections may considerably offset the gain obtained due to the model reduction.

Several approaches were suggested in order to treat non-linearities in an efficient way. Chaturantabut and Sorensen introduced the Discrete Empirical Interpolation Method (DEIM)[12] in order to treat non-linearities in POD-based ROMs governed by systems of time-dependent partial differential equations (PDE). POD-DEIM has become one of the most widely used ROM methods applied to reservoir simulation problems [13, 14]. Carlberg et al. developed the Gauss-Newton with Approximated Tensors (GNAT) method [15] which also uses POD in order to reduce the vector of unknowns, but in contrast to DEIM it operates in a fully discrete domain. Jiang and Durlofsky successfully applied the GNAT approach to complex reservoir simulations [16]. Rewienski and White developed a method called trajectory piecewise linearization (TPWL) [17]. In this method, a number of the system's states and Jacobians are first calculated and saved, then new simulations are obtained as a result of linear expansions around previously saved states. This approach can also be applied in a reduced subspace such as the one obtained through POD. A combination of POD and TPWL (POD-TPWL) is now widely used in order to model subsurface flows [18, 19]. Trehan and Durlofsky [20] developed an extension of TPWL called trajectory piece-wise quadratic extension procedure (TPWQ) and combined it with POD (POD-TPWQ).

In recent years, ROM methods using machine learning (ML) have as well been actively explored. Kani and Elsheikh developed a deep residual recurrent neural network (DR-RNN) approach [21] and applied it to modeling of two-phase subsurface flows [22]. They used POD to project the original problem onto a reduced subspace and applied a recurrent neural network (RNN) in order to model the dynamics in the reduced space. Another group of methods use Variational Autoencoders (VAE) in order to obtain a reduced representation of model's states. Lee and Carlberg [23] modified the GNAT approach and used VAE instead of POD. Temirchev et al. [24] used VAE combined with RNN in order to mimic the dynamics of subsurface flows. In [25], an approach called Neural Differential Equations based ROM (NDE-b-ROM) was suggested: the authors applied the Neural Ordinary Differential Equations method [26] to model the dynamics in the reduced latent space, while the reduced representation was obtained with the help of VAE. Fraces et al. applied feedforward neural networks to approximate derivatives in Buckley-Leverett problem[27]. They used transfer learning approach and Generative Adversarial Networks to obtain continuous in both time and space approximation of PDE solution.

A number of important reservoir engineering problems involve iterative simulations whose total computational cost may be particularly high. A typical example of such problems are various optimization tasks, such as finding the optimal well locations, well geometries, well completion schemes, and well control schedules. Numerical solution of such optimization problems requires multiple simulations of essentially the same reservoir unit with varying well parameters and schedules. Reduced reservoir models including POD-based ROMs, were successfully applied to well control optimization problems [28, 29, 20, 30, 18, 19]. However, some reservoir optimization problems require simulations with varying well locations and well geometries, in addition to different well control sequences. For such problems, standard POD-based ROMs fail to correctly reproduce the flow dynamics even after a slight change in well location or well geometry with respect to the model used to construct the basis. In such cases, classical POD schemes require the construction of a new POD basis after every change in well locations or geometry. That implies re-calculating from scratch of a new training data set based on high-resolution model simulations with a significant associated computational overhead.

In this paper, a POD-based adaptive scheme that allows us to account for changes in well location and well geometry at the expense of a relatively small computational overhead is introduced. The proposed scheme requires significantly less training data compared to what is necessary for constructing a new POD-basis from scratch.

This paper proceeds as follows. In Sect. 2, the governing equations for a two-phase immiscible displacement problem are presented together with an overview of POD-Galerkin ROM method and its application to this problem. In Sect. 3, a test problem related to the optimization of the geometry of a horizontal production well is set up, and two different approaches for construction of the POD-basis for such kind of problems are described. The results of simulations using full resolution and adaptive POD models are compared and discussed. In Sect. 4, advantages and shortcomings of the proposed adaptive POD scheme are discussed, and directions for further work are suggested.

2 POD-Galerkin ROM of Two-phase Immiscible Flow

2.1 Two-phase immiscible flow

The mathematical model of a two-phase immiscible flow is obtained by combining the system of mass conservation (continuity) equations for fluid phases (oil and water), and Darcy's law for each phase. The continuity equation takes the form

$$\frac{\partial \phi \rho_{o,w} s_{o,w}}{\partial t} - \nabla \cdot (\rho_{o,w} \mathbf{v}_{o,w}) + q_{o,w} = 0, \quad (1)$$

where subscript o, w denote oil and water phase respectively, ϕ is the porosity, ρ - the fluid density, s - the fluid saturation, and \mathbf{v} is the Darcy velocity that can be expressed as follows

$$\mathbf{v}_{o,w} = -\lambda_{o,w} \mathbf{K} \nabla (p_{o,w} - \rho_{o,w} g h). \quad (2)$$

Here \mathbf{K} is the absolute permeability tensor, $\lambda = \frac{k_r}{\mu}$ - the phase mobility, k_r is the relative permeability of the corresponding phase, and μ is the viscosity of this phase, p - the fluid pressure, g - the gravitational acceleration, h - the depth, and q is the source or sink term [22]. After neglecting the capillary pressure, compressibility and gravitational effects, mass conservation equation and Darcy's law are combined in order to obtain a system of equations for the global pressure

$$\nabla \cdot \mathbf{K} \lambda \nabla p = q, \quad (3)$$

and for the saturation of the water phase

$$\phi \frac{\partial s_w}{\partial t} + \nabla \cdot \mathbf{v}_w = \frac{q_w}{\rho_w}, \quad (4)$$

where $p = p_o = p_w$ is the global pressure, $\lambda = \lambda_w + \lambda_o$ - the total mobility, $q = q_w + q_o$ - is the source or sink term. The discrete form of the model can be obtained by dividing the domain into blocks and by applying the finite volume method to Eqs. (3) and (4). Discretized pressure equation takes the form

$$\mathbf{A} \mathbf{s}_p = \mathbf{b}, \quad (5)$$

where $\mathbf{A} \in \mathbb{R}^{n \times n}$ is a coefficient matrix, $\mathbf{s}_p \in \mathbb{R}^n$ is the pressure state vector, and $\mathbf{b} \in \mathbb{R}^n$ is the right hand side of the equation. Each element of the unknown vector s_{p_i} represents the mean pressure value in the i -th grid block. Saturation equation takes the form

$$\frac{d\mathbf{s}_s}{dt} + \mathbf{B}(\mathbf{v}) f_w(\mathbf{s}_s) = \mathbf{d}, \quad (6)$$

where $\mathbf{s}_s \in \mathbb{R}^n$ is the saturation state vector, $\mathbf{v} \in \mathbb{R}^n$ is the velocity vector, obtained from the pressure field, $\mathbf{B} \in \mathbb{R}^{n \times n}$ is a coefficient matrix depending on the velocity vector, $f_w(\mathbf{s}_s)$ is the nonlinear term depending on the saturation field, and $\mathbf{d} \in \mathbb{R}^n$ is right hand side of the equation. Equations (5) and (6) are coupled through a dependence of matrix \mathbf{A} on the saturation field and through a dependence of the velocity \mathbf{v} on the pressure field. There are several ways of constructing the numerical solution of such coupled problems. In the present work, the IMPES method [31] is used: at each time step, the saturation field from the previous time step is used to construct the matrix \mathbf{A} . The pressure equation is solved using an implicit scheme in order to obtain the pressure field. The obtained pressure field is then used to calculate the velocity field \mathbf{v} and construct the matrix \mathbf{B} . After that Eq. (6) is solved explicitly and the saturation field is obtained.

2.2 POD-Galerkin model

2.2.1 POD basis

The main objective of proper orthogonal decomposition is to obtain an optimal low dimensional functional basis that is capable to adequately represent high dimensional data. Once constructed, the POD basis can be used in order to formulate a reduced order model that corresponds to the original high resolution model. POD decomposes a given fluctuating field into an orthonormal system of spatial modes $\mathbf{u}_i(x)$ and the corresponding temporal coefficients $a_i(t)$ [32]

$$\mathbf{u}'(x) = \sum_{i=1}^N a_i \mathbf{u}_i(x). \quad (7)$$

The discrete variant of POD is also known as principal component analysis (PCA), and both methods are closely related to singular value decomposition method (SVD) [33]. In order to generate a set of POD modes, the data set should be presented as a matrix \mathbf{X} , where each row represents the variable field at a given instant, such that if the field state is represented by n values, and the data set consists of m field states, then $\mathbf{X} \in \mathbb{C}^{m \times n}$.

The optimality of the POD basis means that for any given dimensionality of the basis r , the truncation error is minimal

$$\int_t \int_x \left(u(x, t) - \sum_{i=1}^r a_i(t) u_i(x) \right)^2 = \min_{\phi, b} \int_t \int_x \left(u(x, t) - \sum_{i=1}^r b_i(t) \phi_i(x) \right)^2. \quad (8)$$

In the discrete case, this equation can be written as

$$\sum_{i=1}^n \sum_{j=1}^m \left(x_{i,j} - \sum_{k=1}^r (u_i^k a_j^k) \right)^2 = \min_{\phi, b} \sum_{i=1}^n \sum_{j=1}^m \left(x_{i,j} - \sum_{k=1}^r (\phi_i^k b_j^k) \right)^2, \quad (9)$$

where $x_{i,j}$ corresponds to the j -th value of the i -th state representation, u_i^k is the i -th value of the k -th basis vector \mathbf{u}^k , and a_j^k is a projection of the j -th field state onto the k -th basis vector. This result can be obtained by the factorization of matrix \mathbf{X} using SVD

$$\mathbf{X} = \mathbf{U} \mathbf{\Sigma} \mathbf{V}^*, \quad (10)$$

where $\mathbf{U} \in \mathbb{C}^{n \times n}$ is the left singular matrix, $\mathbf{V} \in \mathbb{C}^{n \times n}$ is the right singular matrix, $\mathbf{\Sigma} \in \mathbb{R}^{m \times n}$ is the singular matrix (a diagonal matrix with non negative values σ_i on the main diagonal). In matrix form the factorization (10) can be written as

$$\mathbf{X} = \begin{bmatrix} \mathbf{u}_1 & \dots & \mathbf{u}_i & \dots & \mathbf{u}_m \end{bmatrix} \begin{bmatrix} \sigma_1 & & & & \\ & \ddots & & & \\ & & \sigma_i & & \\ & & & \ddots & \\ & 0 & \dots & \dots & 0 \end{bmatrix} \begin{bmatrix} \mathbf{v}_1^* \\ \vdots \\ \mathbf{v}_i^* \\ \vdots \\ \mathbf{v}_n^* \end{bmatrix}, \quad (11)$$

where \mathbf{u}_i is an m -dimensional column vector, and \mathbf{v}_i^* is a n -dimensional row vector. The singular matrix σ is constructed such that $\sigma_1 \geq \sigma_2 \geq \dots \geq 0$ [8]. The optimal reduced basis is obtained by taking the first r left singular vectors \mathbf{u}_i .

In order to obtain a reduced POD basis for a specific problem, one needs to construct a "snapshot" matrix \mathbf{X} which is composed of state vectors s obtained from the solution of the full system. For two- or three-dimensional problems, the model's states are first flattened to vectors. These vectors, called snapshots, are then stacked to compose the snapshot matrix. The reduced POD basis is obtained by applying SVD to the snapshot matrix and keeping the first r columns of the calculated singular matrix.

2.2.2 POD-Galerkin ROM

POD-Galerkin ROM of a two-phase immiscible displacement in IMPES formulation can be stated as follows. During the offline stage (also called the training stage), pressure snapshots are recorded, and snapshot matrix \mathbf{X}_p is constructed. Then SVD (10) is applied to the snapshot matrix, and the reduced basis $\mathbf{U}_p^r = [\mathbf{u}_1 \dots \mathbf{u}_i \dots \mathbf{u}_r]$ is obtained. During the online stage, a reduced representation of the pressure equation (5) is constructed. It can be written as

$$\mathbf{A}^r \mathbf{s}_p^r = \mathbf{b}^r, \quad (12)$$

where $\mathbf{A}^r = \mathbf{U}_p^{r\top} \mathbf{A} \mathbf{U}_p^r$ is a projection of the matrix equation onto the reduced subspace, $\mathbf{s}_p^r = \mathbf{U}_p^{r\top} \mathbf{s}_p$, and $\mathbf{b}^r = \mathbf{U}_p^{r\top} \mathbf{b}$ are the projections of the state vector and of the right hand side of the equation onto the reduced subspace. This equation is solved in the reduced subspace in order to obtain a new reduced pressure state \mathbf{s}_p^r . It is used to form a full representation of the pressure state $\tilde{\mathbf{s}}_p$, the velocity field $\tilde{\mathbf{v}}$, and the coefficient matrix $\mathbf{B}(\mathbf{v})$. The saturation field $\tilde{\mathbf{s}}_s$ is then calculated explicitly, and a new coefficient matrix $\tilde{\mathbf{A}}$ is formed. This procedure is repeated for the subsequent time steps.

3 Well orientation optimization using POD-Galerkin ROM

3.1 Test problem setup

Let us consider a simplified production optimization problem in which one needs to optimize the orientation (azimuth) of a horizontal producing section of a well. A two-dimensional immiscible displacement problem in a square domain of the size 1000×1000 m is considered, and the domain is divided into 40×40 square cells. Heterogeneous porosity and permeability fields are generated numerically in order to mimic a high permeability fluvial channel crossing a less permeable formation (fig. 1). In the corners of the square area are placed four injector wells that inject water at a

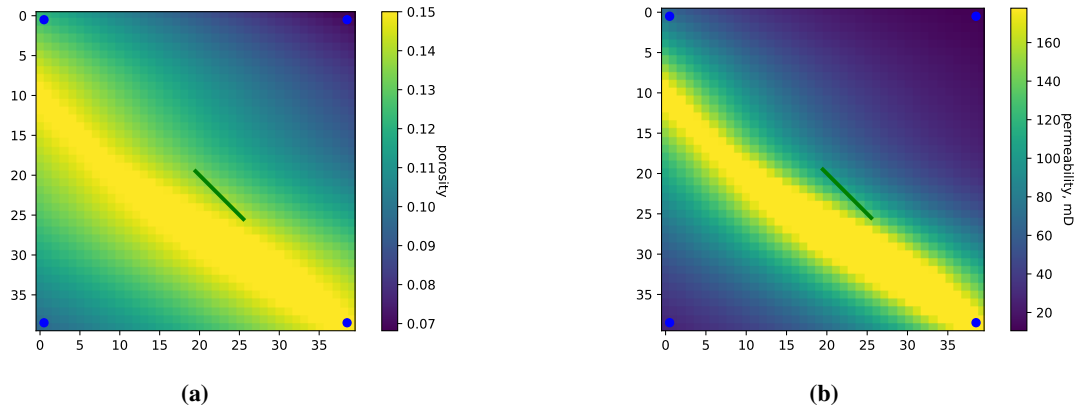


Figure 1 – a - porosity field, b - permeability field of the model; blue dots in the corners indicate the positions of injector wells, green line shows the location of the producer.

controlled injection pressure. The oil that initially saturates the model is displaced toward the center of the simulation area where fluids are recovered by a 150 meter long horizontal producer (fig. 1).

3.2 Universal POD-basis

In order to address optimal well placement problems, the POD-Galerkin model must be capable of simulating production scenarios with various well locations and geometries. Such a "universal" model thus needs to capture the key spatio-temporal features of all these scenarios. This can be achieved by generating a sufficiently long learning data set that contains the maximum amount of information regarding possible modes of the model, or projections of the solutions on the POD basis. In order to generate such a data set, a simulation in which the orientation (azimuth) of the horizontal producer was randomly changed at regular time intervals was recorded. The injection pressure at each injection well was also varied randomly through the simulation. All the pressure fields obtained from this simulation were flattened into vectors and stacked together to form a "snapshot" matrix, where each column represents a specific pressure field state. Singular value decomposition was performed on this matrix (10), and the first r columns of the resulting left singular matrix \mathbf{U} were taken in order to obtain the reduced POD-basis. In figure 2, the first 12 components of the resulting reduced basis are shown. This basis was further used to formulate the reduced problem (12). In Figs. 3 and 4 the simulated fluid production rates for two particular producer orientations (63 and 175 degrees clockwise from the horizontal axis) are shown. One can observe that in both cases the production curves simulated by the reduced model demonstrate a very close match with the solutions obtained by the full model. However, due to the complex spatio-temporal structure of the solutions used for constructing the POD-basis, a relatively large number of components (80-100) of the reduced basis have to be kept in order to achieve such an accuracy. In Fig. 5 the results of modeling of the production rates with different numbers of the reduced basis components are presented.

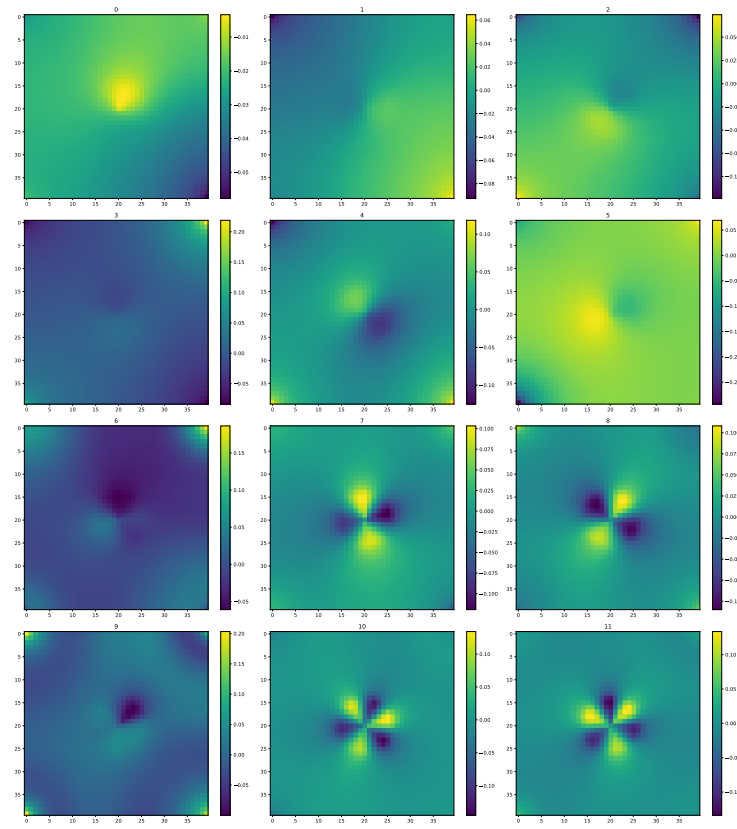


Figure 2 – The first 12 principal components of the universal POD basis.

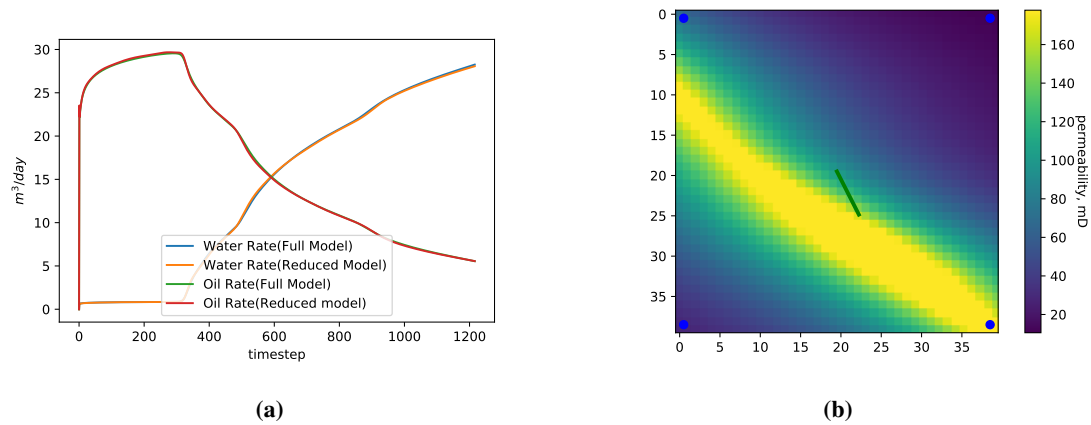


Figure 3 – Simulation of the fluid production of the well oriented 63 degrees clockwise from the horizontal axis. a - production rates, b - well placement scheme

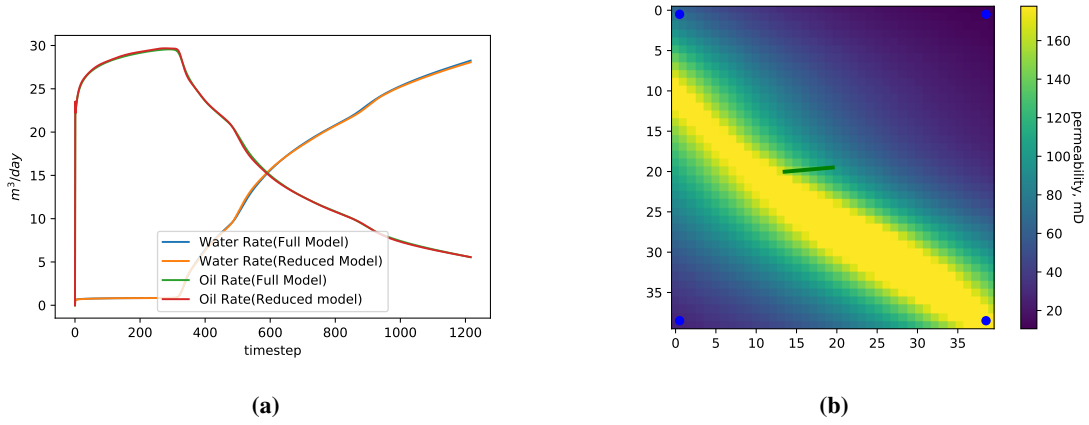


Figure 4 – Simulation with the producer oriented 175 degrees clockwise from the horizontal axis a - production rates, b - well placement scheme

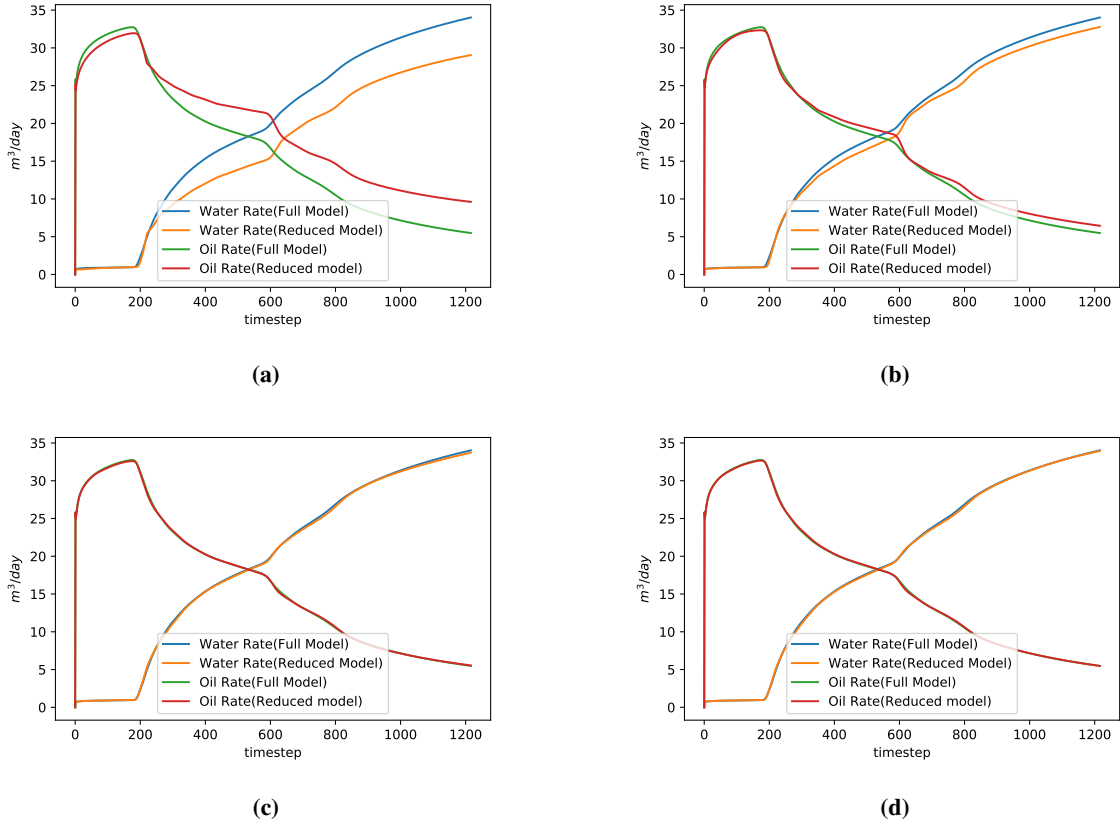


Figure 5 – Production rates simulated using different numbers of components of the reduced basis. a - 20 components, b - 40 components, c - 100 components, d - 120 components.

Root relative squared errors (RRSE) (13) were calculated for the deviation of the solutions obtained with different numbers of the reduced basis components with respect to the full model solution. RRSE is designed to be relative to an error of a simple predictor (constant mean value) [34].

$$E = \sqrt{\frac{\sum_{i=1}^n (\hat{q}_i - q_i)^2}{\sum_{i=1}^n (q_i - \bar{q}_i)^2}}, \quad (13)$$

where \hat{q} - production rate calculated by ROM, q - reference production rate (from full-scale model), \bar{q} - mean value of reference production rate. Errors were calculated separately for oil and water rates. RRSE for oil and water production rates as a function of number of the POD basis components are shown in Fig. 6.

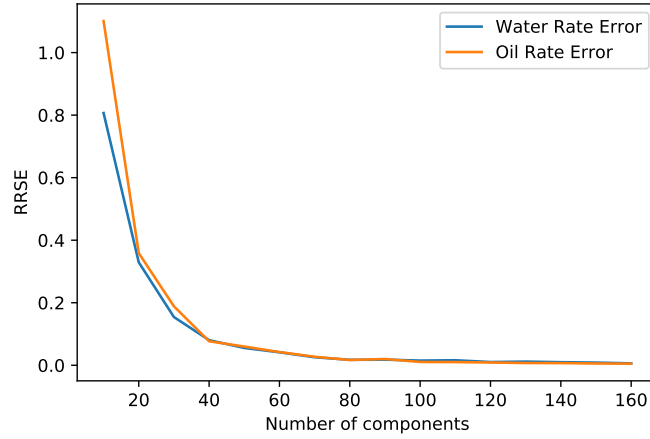


Figure 6 – Root relative squared error of the simulated fluid production rates as a function of number of the POD basis components.

One can observe that a POD basis containing at least 80 components should be used in order to accurately simulate the production rates.

3.3 Adaptive POD basis

3.3.1 Local POD basis

Let us compare the universal basis approach with the construction of the POD-basis for a specific well configuration. The latter is referred in this work as the local basis approach. In this approach, a series of snapshots is generated in the same way as in the universal basis case, however the geometry and the locations of the wells are fixed while the regimes of the injector wells are randomly changed. These snapshot are flattened and stacked into a matrix, after which SVD is applied to that matrix, and the reduced basis is obtained. It should be noted that such a local POD basis is only suitable for simulating scenarios with the specific well configuration for which it was constructed. In Fig. 7, the first 12 principal components of such a local POD-basis for a model with the producer oriented 63 degrees clockwise from the horizontal axis are presented.

In Fig. 8 the simulated production rates obtained using different number of components of the local POD basis are shown.

One can observe that with the local POD-basis, a similar accuracy of the simulations is obtained with fewer POD basis components. For example, simulations with 20 components of the local POD-basis (Fig. 8b) give practically the same accuracy as those with 100 components of the universal POD basis (Fig. 5c) at a significantly lower computational cost. Another advantage of the local basis is that it is much easier to construct since it requires significantly less additional snapshots compared to the original full basis. However, POD-Galerkin model with a local basis is only capable of simulating scenarios with one specific well location and geometry, and if one needs to simulate a new well configuration it is necessary to build a new basis corresponding to that configuration. In Fig. 9 the simulated

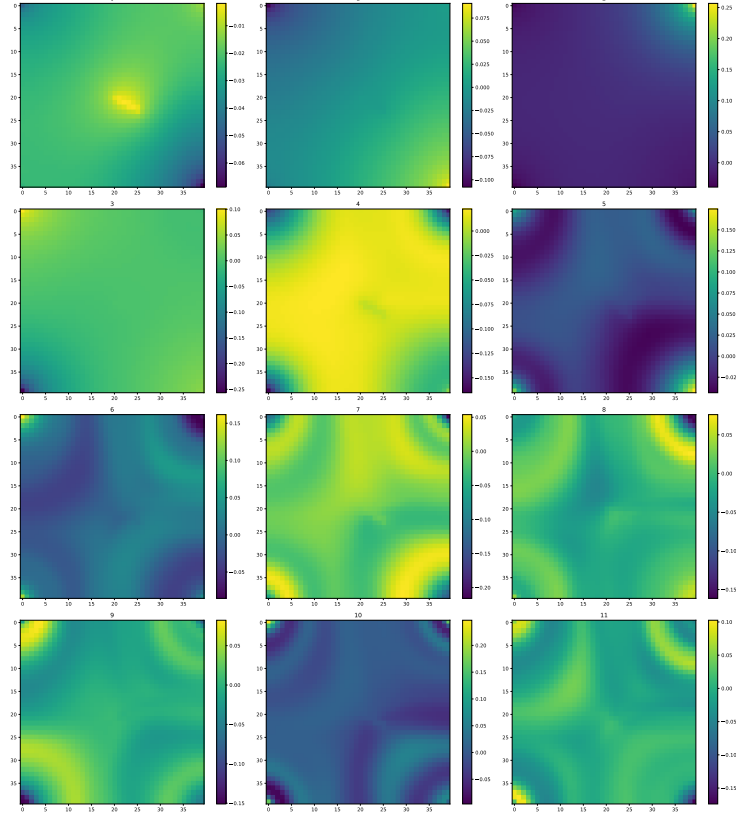


Figure 7 – The first 12 principal components of the local POD basis.

production rates for a well oriented at 175 degrees obtained with the POD basis constructed for a mismatching well orientation (63 degrees clockwise from the horizontal axis) and with different number of the basis components are presented.

One can see that in this case, the simulated production curves do not match the full model solution, and the quality of the simulation remains poor even when using up to 200 POD basis components.

3.3.2 Adaptive POD basis

Although using the local POD basis constructed for a well configuration that does not match the simulated well configuration yields quite poor results, such a mismatching basis still contains some useful information about the simulated problem. In this section, a new approach based on utilization of this information is described which allows us to update the POD basis and make it properly handle simulations with new well configurations. In order to make the old POD basis applicable to a new problem, one needs to update it with additional components while keeping the information about the generic features of the model. Let us suppose that one has the local POD basis constructed for a particular well configuration and needs to simulate production scenarios for different well configurations. Building a new local POD basis from scratch may require a lot of additional computations since one needs to generate a new training data set that typically consists of thousands of simulated snapshots of the full resolution model. Additional computing resource required to generate such a training data set may entirely offset the gains achieved due to POD model reduction and thus make its use meaningless. The proposed approach is based on updating the existing POD basis with a few new components obtained from a limited amount of new snapshots, and allows us to produce accurate simulations with new well configurations using the updated POD basis.

Let us consider a reduced POD basis \mathbf{U}_o^r constructed for a given well configuration, and calculate a few additional snapshots corresponding to the new well location \mathbf{s}_{p_i} . The information which is lost by projecting these snapshots onto the reduced subspace defined by the basis \mathbf{U}_o^r can be expressed as

$$\mathbf{s}_{p_i}^{res} = \mathbf{s}_{p_i} - \mathbf{U}_o^r \mathbf{s}_{p_i} \mathbf{U}_o^{r\top}, \quad (14)$$

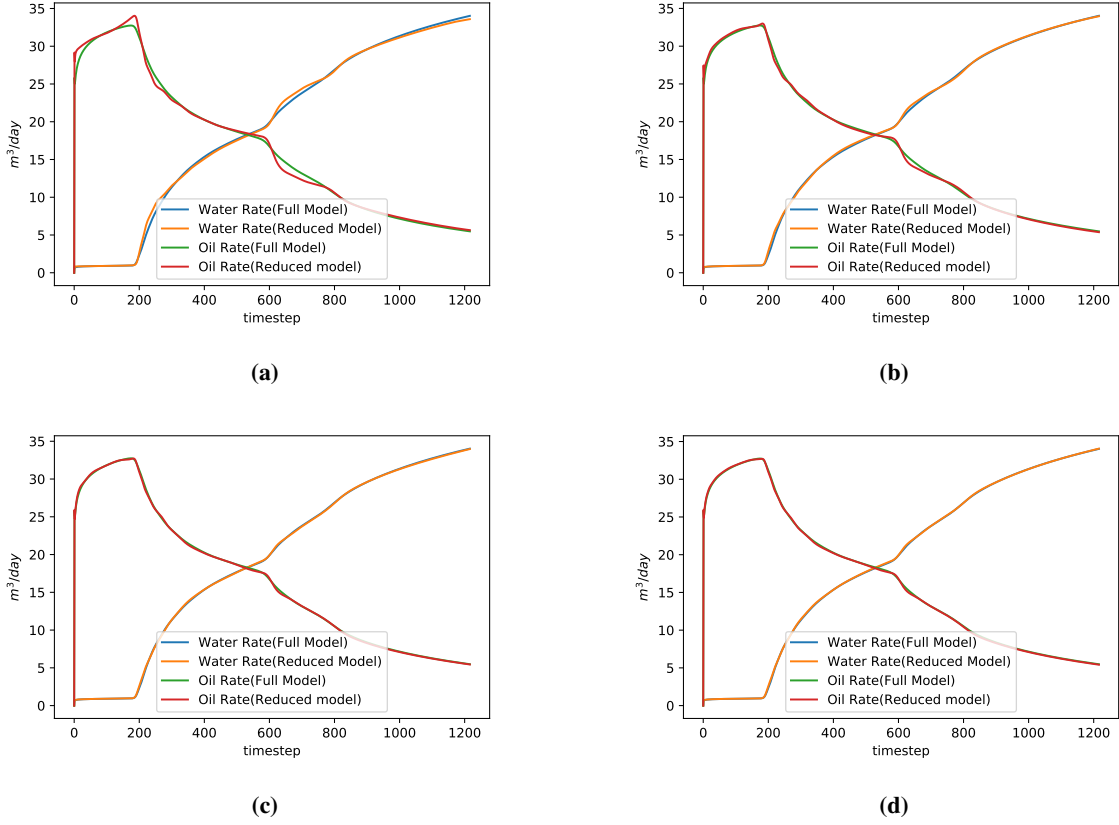


Figure 8 – Production rates simulated using the local POD basis with different number of components. a - 10 components, b - 20 components, c - 30 components, d - 35 components.

or in the matrix form:

$$\mathbf{S}_p^{res} = \mathbf{S}_p - \mathbf{U}_o^r \mathbf{S}_p \mathbf{U}_o^{r\top}. \quad (15)$$

One can then apply SVD to this residual snapshot matrix in order to obtain a residual basis \mathbf{U}_{res}^r . By construction, this basis will be orthogonal to \mathbf{U}_o^r , so that one can use a combination of components from this basis in order to build an updated basis $\tilde{\mathbf{U}}^r$ that can be used in the POD-Galerkin method. The suggested method complements \mathbf{U}_o^r by a few components from \mathbf{U}_{res}^r in order to construct $\tilde{\mathbf{U}}^r$ which can be used in a reduced POD-Galerkin model for the new well configuration. The workflow of the proposed method can be summarized as follows:

1. calculate n snapshots with the new well configuration;
2. compose the snapshot matrix \mathbf{S} ;
3. calculate the residual snapshot matrix \mathbf{S}_p^{res} ;
4. perform SVD and take the first r^{res} components ($r^{res} \ll r$);
5. update the existing POD basis \mathbf{U}_o^r with these components and obtain $\tilde{\mathbf{U}}^r$.
6. Use $\tilde{\mathbf{U}}^r$ to formulate the updated reduced POD-Galerkin model.

Now let us consider an example of the application of the proposed method. As the initial basis, \mathbf{U}_o^r a local basis consisting of 20 components and corresponding to the well oriented 63 degrees clockwise from the horizontal axis (Fig. 7) is taken. Only 10 additional snapshots for the new well direction (175 degrees clockwise from the horizontal axis) are simulated. As a reminder: construction from scratch of a new POD basis for that problem would require generating about a thousand snapshots. The snapshot matrix \mathbf{S}_p is then composed, and the residual snapshot matrix \mathbf{S}_p^{res} is obtained using (15). In Fig. 10 one of such snapshots, the corresponding reduced snapshot ($\mathbf{U}_o^r \mathbf{S}_{p_i} \mathbf{U}_o^{r\top}$), and the residual snapshot (14) are shown. SVD is then performed on the residual snapshot matrix, and the additional

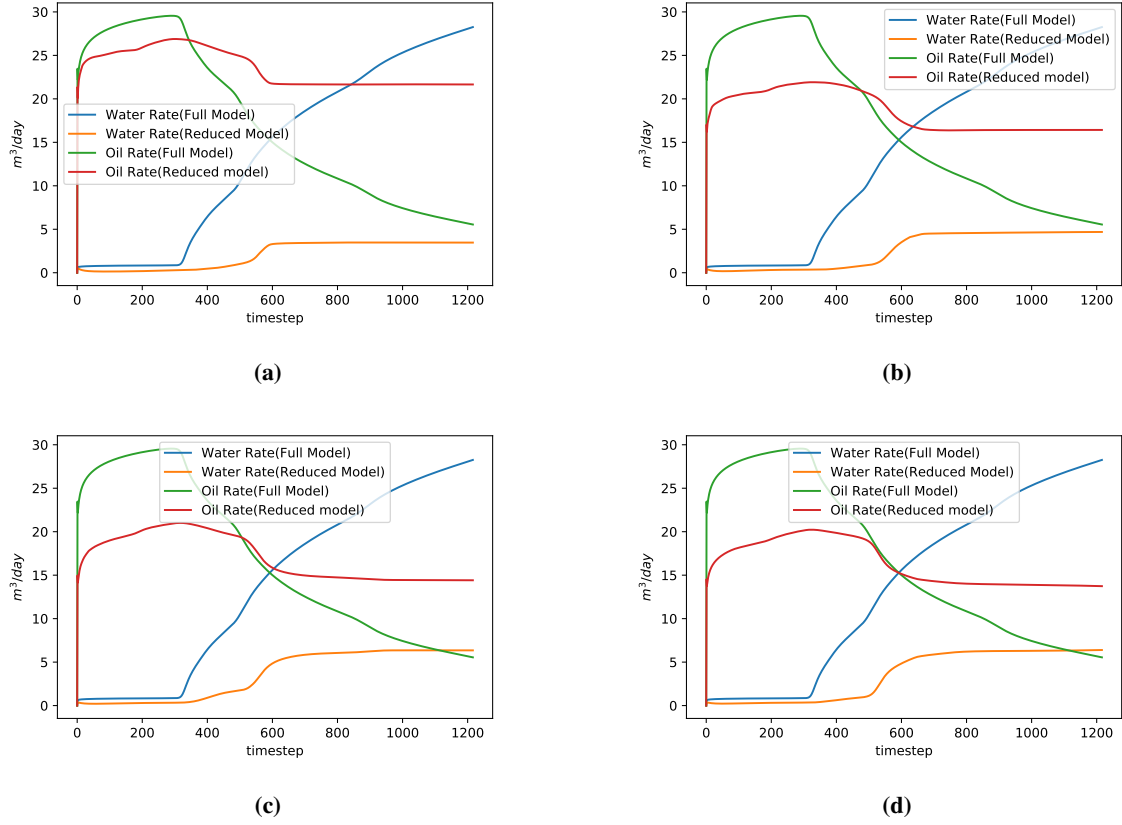


Figure 9 – Simulated production rates of the well oriented 175 degrees clockwise from the horizontal axis using the local POD basis constructed for a mismatching producer orientation (63 degrees) and a different number of components of the reduced basis: a - 20 components, b - 40 components, c - 100 components, d - 200 components.

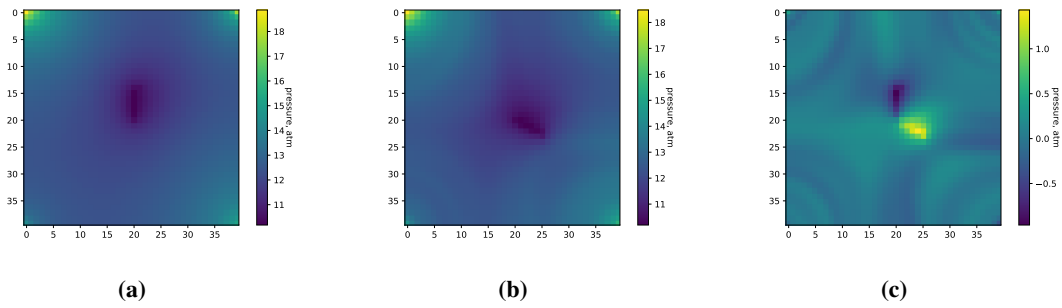


Figure 10 – a - original snapshot (s_{p_i}), b - reduced snapshot ($U_o^r s_{p_i} U_o^{r\top}$), c - residual snapshot (S_p^{res}).

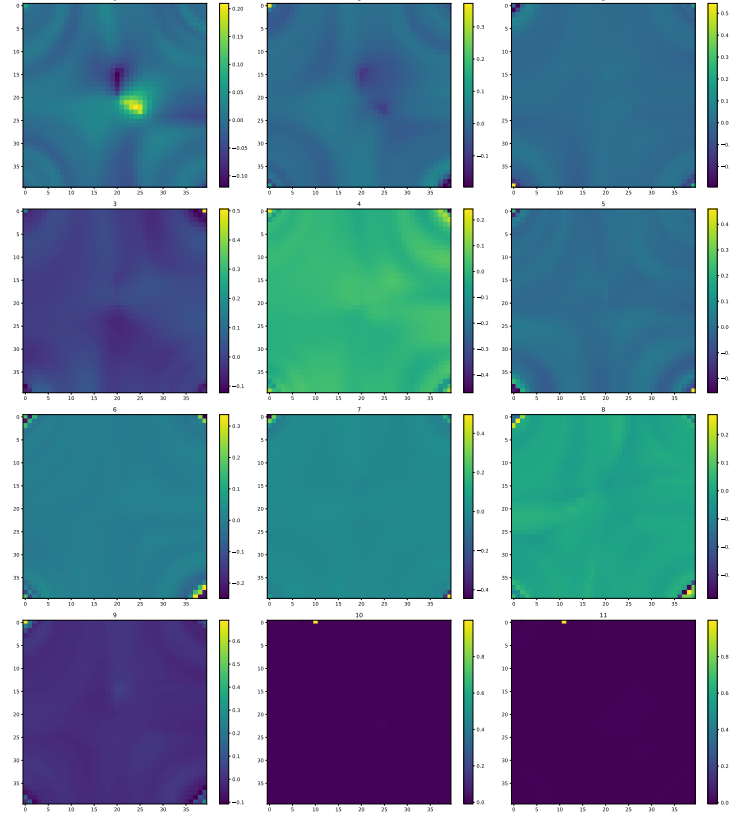


Figure 11 – The first 12 principal components of the residual snapshot matrix decomposition (\mathbf{U}_{res}^r).

components are obtained. The first 12 of the resulting additional components are presented in the Fig. 11. Since only 10 additional snapshots were used, most of the higher order residual components are quite noisy and contain little structural information about the model. Consequently, only the first three residual components will be used to build the updated basis $\tilde{\mathbf{U}}^r$ by adding them to the original basis \mathbf{U}_o^r . One can then use the updated basis to formulate the POD-Galerkin problem for the new well configuration. The simulated production rates obtained for the new well configuration with the updated POD basis are shown in Fig. 12. One can observe that the proposed method of the

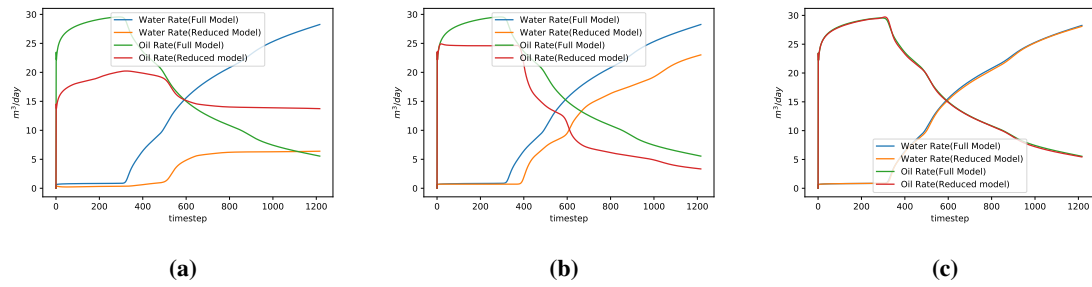


Figure 12 – Simulated fluid production rates: a - using the local basis for a mismatching well orientation; b - using the updated POD basis constructed from 10 additional snapshots; c - using the adaptive POD basis.

local basis adaptation significantly increases the accuracy of the simulations. In Fig. 12b, the results of simulation of the production rates using the local basis with 23 components (the same number as in the adaptive basis) built using the same 10 additional snapshots, are presented. One can conclude from these simulations that 10 additional snapshots of the model are not sufficient to construct a new basis without using the information contained in original basis. However, the adaptive POD-basis scheme with the same 10 additional snapshots provides quite a satisfactory result.

In order to estimate the number of snapshots required to build the local basis from scratch, a number of simulations with POD-Galerkin models using bases constructed from varying numbers of snapshots were performed. The corresponding simulated production rates are shown in Fig. 13. One can observe that in order to construct a proper local

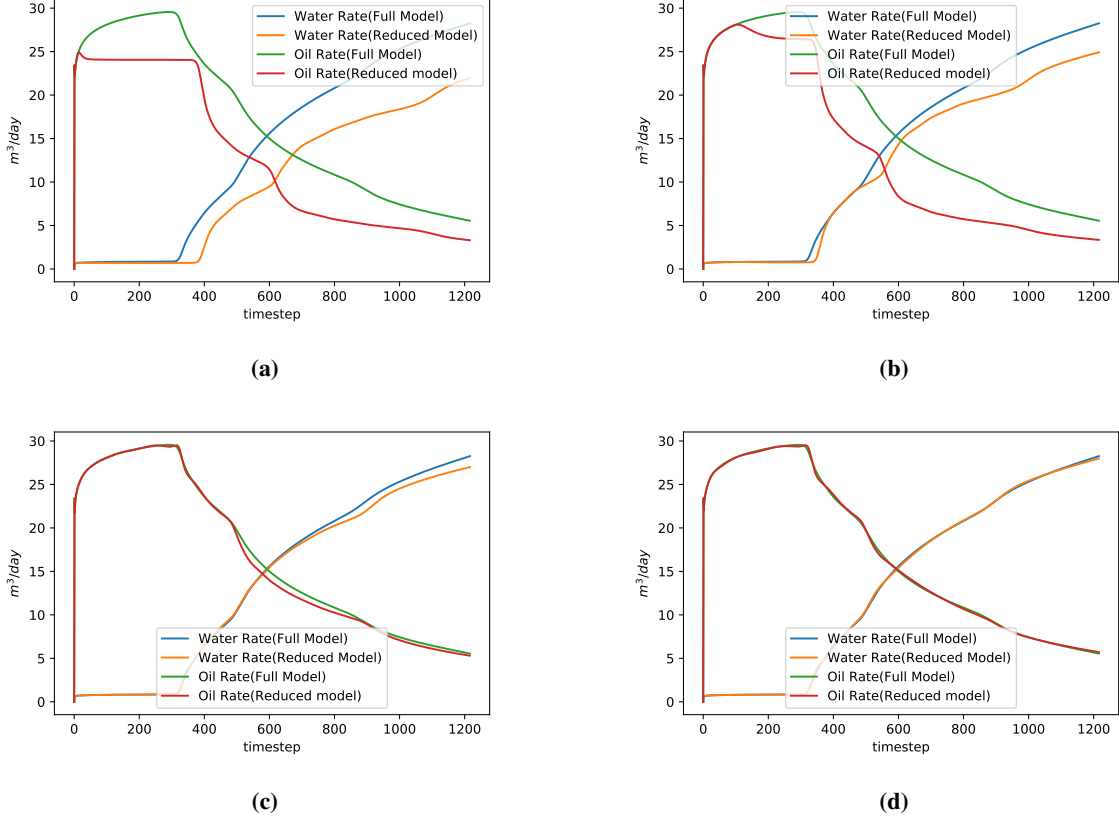


Figure 13 – Production rates simulated using POD-Galerkin models with local bases constructed from different number of snapshots: a - 10 snapshots; b - 100 snapshots; c - 500 snapshots; d - 1000 snapshots.

basis, about 1000 snapshots are required, in contrast with just about 10 additional snapshots needed for the adaptation of the existing basis.

3.3.3 Adaptive POD bases for models with variations of well location and well length

In order to further test the applicability of the proposed technique to problems with changing well configurations, it was used to build the adaptive bases for models with variations of well location and well length. In Fig. 14, the well location for which the original POD basis was constructed, as well as the new location for which the adaptation of the original basis will be performed are presented. In Fig. 15, a comparison of the simulated fluid production rates for the new producer location is shown for models using the original POD basis and the adaptive POD basis.

In Fig. 16, a well placement scheme with the variation of the length of the producing section is shown. In Fig. 17, a comparison of the simulated fluid production rates for this model obtained with the use of the original POD basis and with the adaptive POD basis is presented.

One can see that the proposed approach allows us to adapt the existing ROM to a wide range of new well configurations, including varying well orientations, length, and position at the expense of a relatively small number of additional snapshots. In contrast, if one tries to build an universal POD-based ROM capable of accurately simulating production rates for models with variable well positions and geometries, a set of snapshots that scales exponentially with the number of varying parameters (well orientation, well length, etc.) is required. In statistics and in ML applications this problem is known as the curse of dimensionality [35]. Another problem that one would face in this case, is an increasing complexity of the snapshots space that would in turn lead to a significant increase of the number of

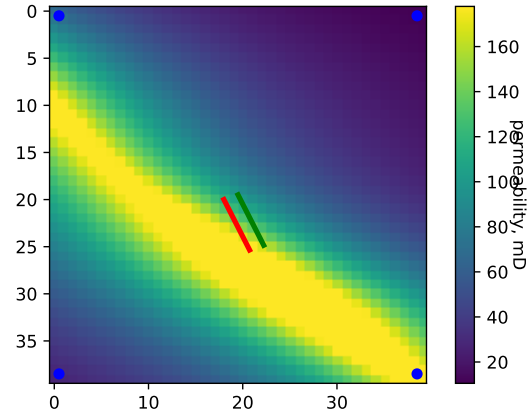


Figure 14 – Well placement scheme: blue circles represent the injector wells; the green line represents the original position of the producer; the red line represents the new position of the producer.

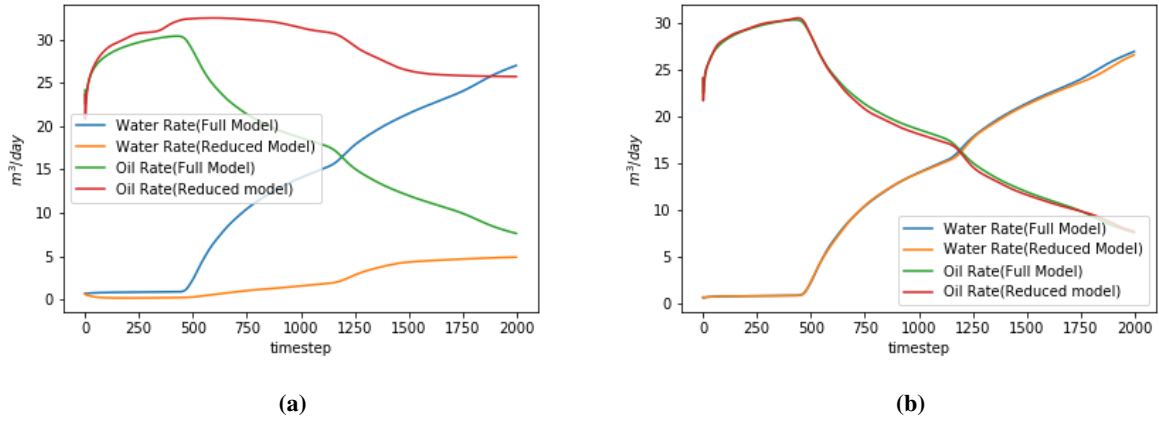


Figure 15 – Simulated fluid production rates: a - the original POD basis, b - the adaptive POD basis constructed using 50 new snapshots and 1 additional component.

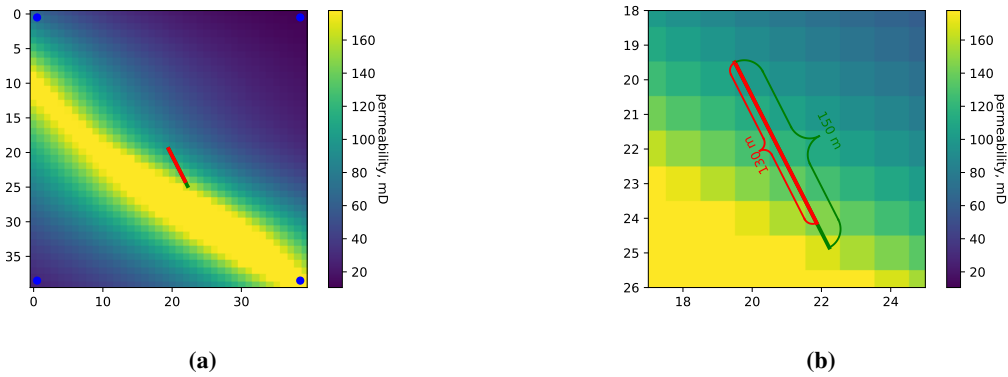


Figure 16 – a - Well placement scheme. Blue circles represent the injector wells; the green line shows the original position and length of the producer; the red line indicates the new length of the producer. b - zoomed in part of the model with the producer well.

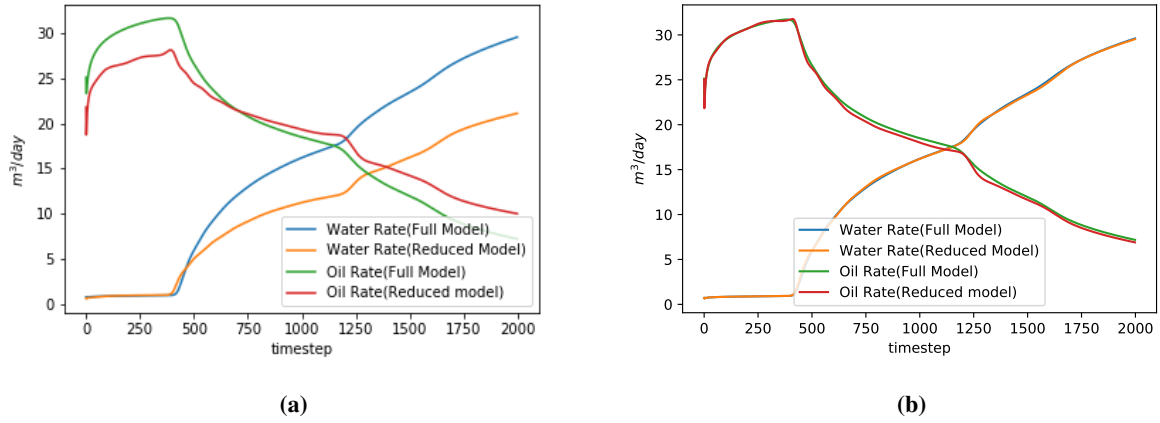


Figure 17 – Simulated fluid production rates: a - the original POD basis, b - the adaptive POD basis constructed using 50 new snapshots and 1 additional component.

POD basis components required to obtain adequate simulation accuracy and stability. This makes such an approach impractical for problems with multiple optimization parameters.

3.3.4 Sensitivity analysis

In order to estimate the impact of the number of additional snapshots used in the adaptive POD basis on the accuracy of the flow rate simulations, several variants of the model with different lengths of the producer and a different number of additional snapshots for each of the variants (Fig. 16) were simulated. The results of these simulations are presented in Fig. 18.

Deviations of the simulated fluid production rates with respect to the full model were calculated for the models with the adaptive POD basis constructed using different number of additional snapshots. The corresponding RRSE graphs are presented in Fig. 19.

Not surprisingly, the increase of the number of additional snapshots up to 30-50 generally improves the accuracy of the flow rate simulations. However, further increase of the number of additional snapshots beyond that range does not seem to improve the accuracy.

In Fig. 20, the simulated fluid production rates are shown for models using adaptive POD basis with different number of additional components. In all the presented cases, the POD basis adaptation was performed using 50 additional snapshots.

Deviations of the simulated fluid production rates with respect to the full model were calculated for the cases with the adaptive POD basis constructed using different number of additional components. The corresponding RRSE graphs are presented in Fig. 21.

One can observe that the influence of the number of additional components of the adaptive basis on the production rate simulations is relatively small, and typically 1-3 additional components are sufficient for a satisfactory basis adaptation.

4 Summary and Further Work

In this work, different approaches for an efficient use of POD-Galerkin ROMs for the reservoir simulation were explored for problems where changes of the boundary conditions, such as well location and geometry, are essential. In the universal basis approach, a training data set is generated such that it contains snapshots of the solutions related to all the considered well geometries. This approach allows us to use the same POD basis for simulating scenarios with different well geometries. However, that universality comes at the expense of a relatively large number of the POD basis components required in order to obtain a reasonable accuracy of the simulations. Another drawback of this approach is the requirement of a very large training data set that should reflect all the range of possible scenarios. This approach may be relevant in cases where one needs to explore a relatively small range of possible well geometries.

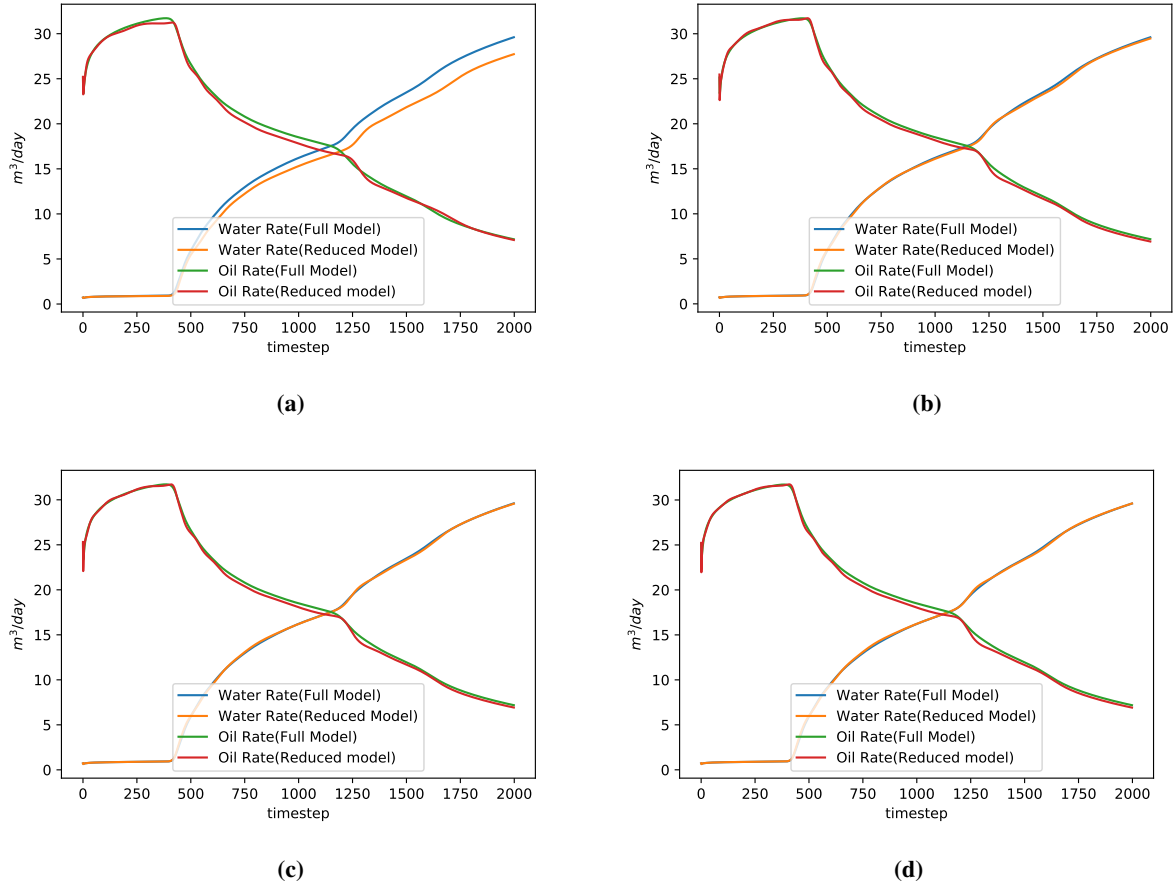


Figure 18 – Simulated fluid production rates for the model with a variable length of the producer, obtained with the adaptive POD basis using different number of snapshots: a - 10 snapshots, b - 30 snapshots, c - 50 snapshots, d - 100 snapshots.

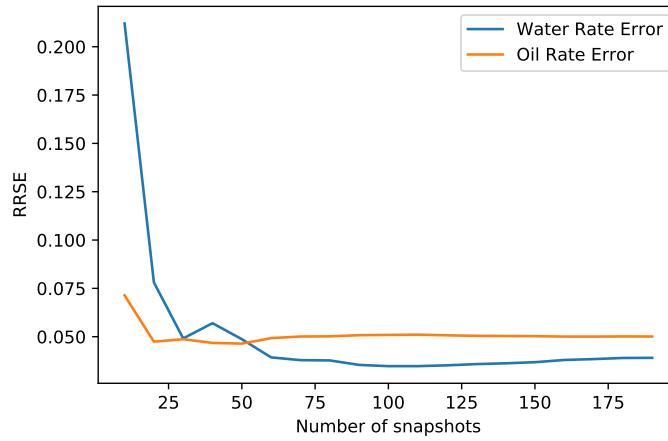


Figure 19 – Root relative squared error of simulated fluid production rates with respect to the full model as a function of number of additional snapshots used in the construction of the adaptive POD basis.

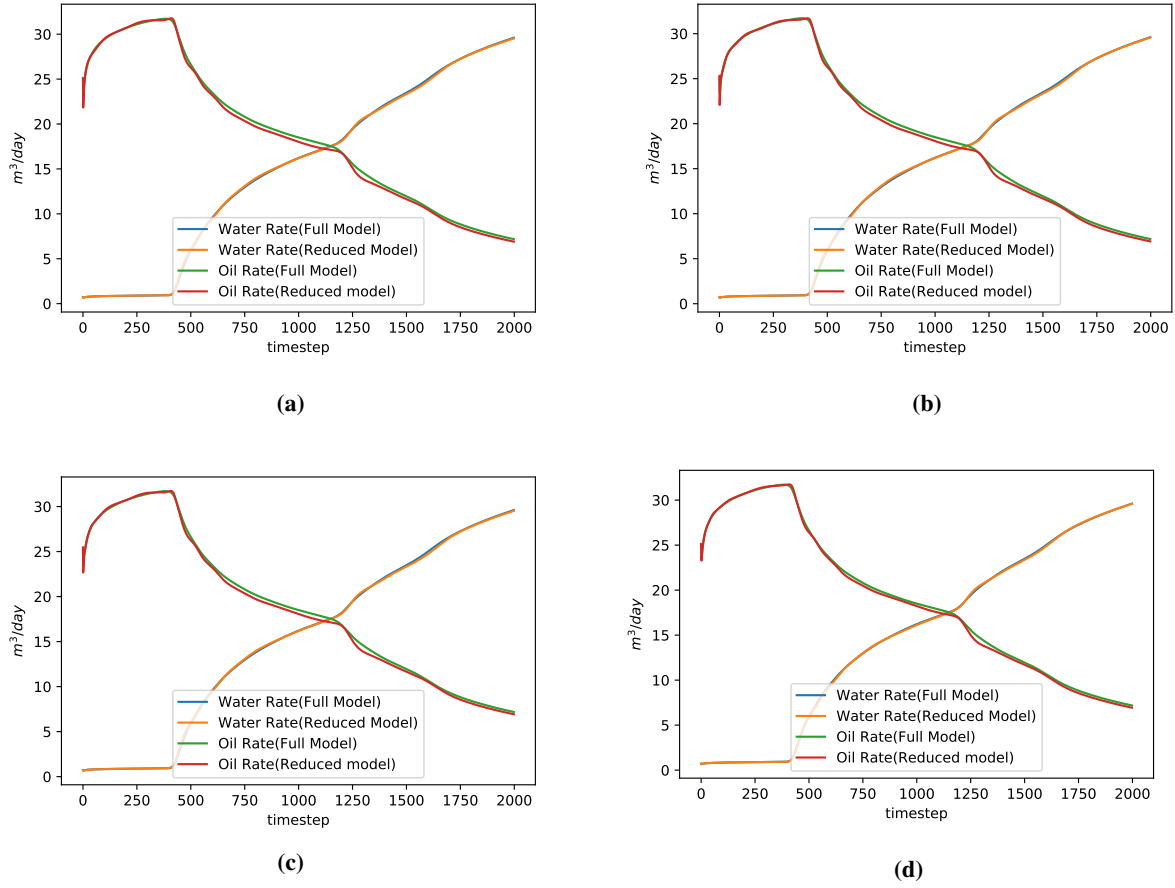


Figure 20 – Simulated fluid production rates for models with the adaptive POD basis with different number of additional components: a - 1 component, b - 3 components, c - 5 components, d - 10 components.

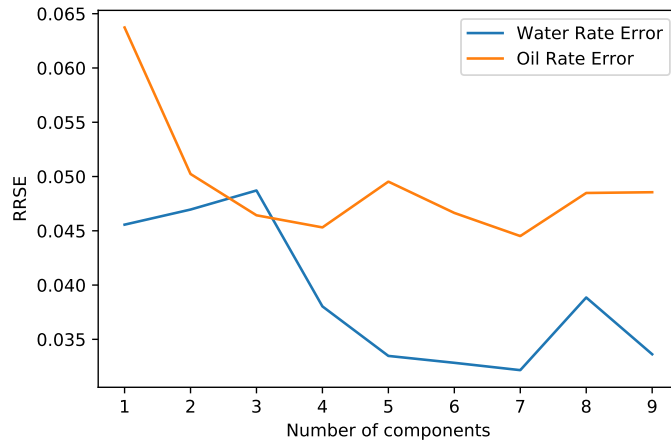


Figure 21 – Root relative squared error of simulated fluid production rates with respect to the full model as a function of the number of additional components of the adaptive POD basis.

A new approach based on the adaptation of the POD basis to varying well configurations was introduced. This approach allows us to use the POD basis constructed for a specific model configuration in order to model a different problem setting. Such an adaptation of the POD basis is achieved at a relatively low computational cost, after updating the basis with a few additional components obtained from the snapshots of the new model configuration. It was found that the number of such additional snapshots is substantially smaller compared to that required for building of a new POD basis from scratch. The new adaptive method was validated on several test cases where a POD-Galerkin ROM was used to simulate immiscible oil displacement by water injection in the model settings where the horizontal producer had variable location, length, and orientation.

So far, the POD reduction technique was applied only to the pressure field. An extension of the proposed adaptive approach to reduce the saturation related part of the model is in the scope of the future work. Another envisaged direction of the work is related to the application of the proposed adaptive POD approach in order to build efficient ROM simulators that are capable to address realistic reservoir optimization problems, such as the optimal well design, completion, and hydraulic fracturing.

References

- [1] Khalid Aziz and Antonín Settari. *Petroleum reservoir simulation*. en. London: Applied Science Publishers, 1979. ISBN: 978-0-85334-787-3.
- [2] J. E. P. Monteagudo and A. Firoozabadi. “Control-volume method for numerical simulation of two-phase immiscible flow in two- and three-dimensional discrete-fractured media”. en. In: *Water Resour. Res.* 40.7 (July 2004). ISSN: 00431397. DOI: 10.1029/2003WR002996. URL: <http://doi.wiley.com/10.1029/2003WR002996> (visited on 03/19/2020).
- [3] Larry C. Young. “A Finite-Element Method for Reservoir Simulation”. en. In: *Society of Petroleum Engineers Journal* 21.01 (Feb. 1981), pp. 115–128. ISSN: 0197-7520. DOI: 10.2118/7413-PA. URL: <http://www.onepetro.org/doi/10.2118/7413-PA> (visited on 03/19/2020).
- [4] K H Coats, L.K. Thomas, and R. G. Pierson. “Compositional and Black Oil Reservoir Simulation”. en. In: *SPE Reservoir Evaluation & Engineering* (1998), p. 8. DOI: <https://doi.org/10.2118/50990-PA>.
- [5] A.G. Spillette, J.G. Hillestad, and H.L. Stone. “A High-Stability Sequential Solution Approach to Reservoir Simulation”. In: *SPE-4542-MS*. Journal Abbreviation: SPE-4542-MS. SPE: Society of Petroleum Engineers, Jan. 1973, p. 14. ISBN: 978-1-55563-773-6. DOI: 10.2118/4542-MS. URL: <https://doi.org/10.2118/4542-MS>.
- [6] Jiamin Jiang and Hamdi A. Tchelepi. “Nonlinear acceleration of sequential fully implicit (SFI) method for coupled flow and transport in porous media”. en. In: *Computer Methods in Applied Mechanics and Engineering* 352 (Aug. 2019), pp. 246–275. ISSN: 00457825. DOI: 10.1016/j.cma.2019.04.030. URL: <https://linkinghub.elsevier.com/retrieve/pii/S0045782519302336> (visited on 07/21/2020).
- [7] Piyush M. Mehta and Richard Linares. “A methodology for reduced order modeling and calibration of the upper atmosphere”. en. In: *Space Weather* 15.10 (Oct. 2017), pp. 1270–1287. ISSN: 15427390. DOI: 10.1002/2017SW001642. URL: <http://doi.wiley.com/10.1002/2017SW001642> (visited on 09/19/2019).
- [8] Eli Shlizerman et al. “The Proper Orthogonal Decomposition for Dimensionality Reduction in Mode-Locked Lasers and Optical Systems”. en. In: *International Journal of Optics* 2012 (2012), pp. 1–18. ISSN: 1687-9384, 1687-9392. DOI: 10.1155/2012/831604. URL: <http://www.hindawi.com/journals/ijo/2012/831604/> (visited on 09/17/2019).
- [9] D. Xiao et al. “Non-intrusive reduced order modelling of the Navier–Stokes equations”. en. In: *Computer Methods in Applied Mechanics and Engineering* 293 (Aug. 2015), pp. 522–541. ISSN: 00457825. DOI: 10.1016/j.cma.2015.05.015. URL: <https://linkinghub.elsevier.com/retrieve/pii/S0045782515001887> (visited on 10/03/2019).
- [10] Weigang Yao et al. “A Reduced-order Model for Aerodynamic Shape Optimization”. en. In: *AIAA Scitech 2019 Forum*. San Diego, California: American Institute of Aeronautics and Astronautics, Jan. 2019, p. 23. ISBN: 978-1-62410-578-4. DOI: 10.2514/6.2019-0975. URL: <https://arc.aiaa.org/doi/10.2514/6.2019-0975> (visited on 09/19/2019).
- [11] Kevin Carlberg, Matthew Barone, and Harbir Antil. “Galerkin v. least-squares Petrov–Galerkin projection in nonlinear model reduction”. en. In: *Journal of Computational Physics* 330 (Feb. 2017), pp. 693–734. ISSN: 00219991. DOI: 10.1016/j.jcp.2016.10.033. URL: <https://linkinghub.elsevier.com/retrieve/pii/S0021999116305319> (visited on 07/11/2020).
- [12] Saifon Chaturantabut and Danny C. Sorensen. “Nonlinear Model Reduction via Discrete Empirical Interpolation”. en. In: *SIAM J. Sci. Comput.* 32.5 (Jan. 2010), pp. 2737–2764. ISSN: 1064-8275, 1095-7197. DOI: 10.1137/090766498. URL: <http://epubs.siam.org/doi/10.1137/090766498> (visited on 08/12/2019).
- [13] Xiaosi Tan et al. “Trajectory-based DEIM (TDEIM) model reduction applied to reservoir simulation”. en. In: *Comput Geosci* 23.1 (Feb. 2019), pp. 35–53. ISSN: 1420-0597, 1573-1499. DOI: 10.1007/s10596-018-9782-0. URL: <http://link.springer.com/10.1007/s10596-018-9782-0> (visited on 11/27/2019).
- [14] Yalchin Efendiev, Eduardo Gildin, and Yanfang Yang. “Online Adaptive Local-Global Model Reduction for Flows in Heterogeneous Porous Media”. en. In: *Computation* 4.2 (June 2016), p. 22. ISSN: 2079-3197. DOI: 10.3390/computation4020022. URL: <http://www.mdpi.com/2079-3197/4/2/22> (visited on 11/29/2019).
- [15] Kevin Carlberg, Charbel Bou-Mosleh, and Charbel Farhat. “Efficient non-linear model reduction via a least-squares Petrov-Galerkin projection and compressive tensor approximations”. en. In: *Int. J. Numer. Meth. Engng.* 86.2 (Apr. 2011), pp. 155–181. ISSN: 00295981. DOI: 10.1002/nme.3050. URL: <http://doi.wiley.com/10.1002/nme.3050> (visited on 11/29/2019).
- [16] Rui Jiang and Louis J. Durlofsky. “Implementation and detailed assessment of a GNAT reduced-order model for subsurface flow simulation”. en. In: *Journal of Computational Physics* 379 (Feb. 2019), pp. 192–213. ISSN: 00219991. DOI: 10.1016/j.jcp.2018.11.038. URL: <https://linkinghub.elsevier.com/retrieve/pii/S0021999118307836> (visited on 11/29/2019).

- [17] M. Rewienski and J. White. “A trajectory piecewise-linear approach to model order reduction and fast simulation of nonlinear circuits and micromachined devices”. en. In: *IEEE Trans. Comput.-Aided Des. Integr. Circuits Syst.* 22.2 (Feb. 2003), pp. 155–170. ISSN: 0278-0070. DOI: 10.1109/TCAD.2002.806601. URL: <http://ieeexplore.ieee.org/document/1174092/> (visited on 07/20/2020).
- [18] M.A. Cardoso and L.J. Durlofsky. “Linearized reduced-order models for subsurface flow simulation”. en. In: *Journal of Computational Physics* 229.3 (Feb. 2010), pp. 681–700. ISSN: 00219991. DOI: 10.1016/j.jcp.2009.10.004. URL: <https://linkinghub.elsevier.com/retrieve/pii/S002199910900549X> (visited on 11/19/2019).
- [19] J. He, J. Sætrum, and L.J. Durlofsky. “Enhanced linearized reduced-order models for subsurface flow simulation”. en. In: *Journal of Computational Physics* 230.23 (Sept. 2011), pp. 8313–8341. ISSN: 00219991. DOI: 10.1016/j.jcp.2011.06.007. URL: <https://linkinghub.elsevier.com/retrieve/pii/S0021999111003561> (visited on 12/03/2019).
- [20] Sumeet Trehan and Louis J. Durlofsky. “Trajectory piecewise quadratic reduced-order model for subsurface flow, with application to PDE-constrained optimization”. en. In: *Journal of Computational Physics* 326 (Dec. 2016), pp. 446–473. ISSN: 00219991. DOI: 10.1016/j.jcp.2016.08.032. URL: <https://linkinghub.elsevier.com/retrieve/pii/S0021999116303898> (visited on 12/03/2019).
- [21] J. Nagoor Kani and Ahmed H. Elsheikh. “DR-RNN: A deep residual recurrent neural network for model reduction”. en. In: *arXiv:1709.00939 [cs]* (Sept. 2017). arXiv: 1709.00939. URL: <http://arxiv.org/abs/1709.00939> (visited on 11/27/2018).
- [22] J. Nagoor Kani and Ahmed H. Elsheikh. “Reduced-Order Modeling of Subsurface Multi-phase Flow Models Using Deep Residual Recurrent Neural Networks”. en. In: *Transport in Porous Media* (Oct. 2018). ISSN: 0169-3913, 1573-1634. DOI: 10.1007/s11242-018-1170-7. URL: <http://link.springer.com/10.1007/s11242-018-1170-7> (visited on 11/27/2018).
- [23] Kookjin Lee and Kevin T. Carlberg. “Model reduction of dynamical systems on nonlinear manifolds using deep convolutional autoencoders”. en. In: *Journal of Computational Physics* (Nov. 2019), p. 108973. ISSN: 00219991. DOI: 10.1016/j.jcp.2019.108973. URL: <https://linkinghub.elsevier.com/retrieve/pii/S0021999119306783> (visited on 12/03/2019).
- [24] P. Temirchev et al. “Deep neural networks predicting oil movement in a development unit”. en. In: *Journal of Petroleum Science and Engineering* 184 (Jan. 2020), p. 106513. ISSN: 09204105. DOI: 10.1016/j.petrol.2019.106513. URL: <https://linkinghub.elsevier.com/retrieve/pii/S0920410519309349> (visited on 12/03/2019).
- [25] Pavel Temirchev et al. “Reduced Order Reservoir Simulation with Neural-Network Based Hybrid Model”. In: *SPE-196864-MS*. Journal Abbreviation: SPE-196864-MS. SPE: Society of Petroleum Engineers, Oct. 2019, p. 17. ISBN: 978-1-61399-692-8. DOI: 10.2118/196864-MS. URL: <https://doi.org/10.2118/196864-MS>.
- [26] Ricky T. Q. Chen et al. “Neural Ordinary Differential Equations”. en. In: *arXiv:1806.07366 [cs, stat]* (Jan. 2019). arXiv: 1806.07366. URL: <http://arxiv.org/abs/1806.07366> (visited on 12/03/2019).
- [27] Cedric G. Fraces, Adrien Papaioannou, and Hamdi Tchelepi. “Physics Informed Deep Learning for Transport in Porous Media. Buckley Leverett Problem”. en. In: *arXiv:2001.05172 [physics, stat]* (Jan. 2020). arXiv: 2001.05172. URL: <http://arxiv.org/abs/2001.05172> (visited on 07/21/2020).
- [28] Jan Dirk Jansen and Louis J. Durlofsky. “Use of reduced-order models in well control optimization”. en. In: *Optim Eng* 18.1 (Mar. 2017), pp. 105–132. ISSN: 1389-4420, 1573-2924. DOI: 10.1007/s11081-016-9313-6. URL: <http://link.springer.com/10.1007/s11081-016-9313-6> (visited on 09/20/2019).
- [29] M A Cardoso. “Use of Reduced-Order Modeling Procedures for Production Optimization”. en. In: *SPE Journal* (2010), p. 10.
- [30] Edwin Insuasty et al. “Tensor-based reduced order modeling in reservoir engineering: An application to production optimization”. en. In: *IFAC-PapersOnLine* 48.6 (2015), pp. 254–259. ISSN: 24058963. DOI: 10.1016/j.ifacol.2015.08.040. URL: <https://linkinghub.elsevier.com/retrieve/pii/S2405896315009076> (visited on 09/20/2019).
- [31] John R. Fanchi. *Principles of applied reservoir simulation*. en. Fourth edition. OCLC: on1013721657. Cambridge, MA, USA: Gulf Professional Publishing is an imprint of Elsevier, 2018. ISBN: 978-0-12-815563-9.
- [32] K. Kunisch and S. Volkwein. “Galerkin Proper Orthogonal Decomposition Methods for a General Equation in Fluid Dynamics”. en. In: *SIAM Journal on Numerical Analysis* 40.2 (2003), pp. 492–515. URL: <http://www.jstor.org/stable/4100966>.
- [33] Hervé Abdi and Lynne J. Williams. “Principal component analysis”. en. In: *WIREs Comp Stat* 2.4 (July 2010), pp. 433–459. ISSN: 19395108. DOI: 10.1002/wics.101. URL: <http://doi.wiley.com/10.1002/wics.101> (visited on 07/11/2020).

- [34] Ian H. Witten and Eibe Frank. *Data Mining: Practical Machine Learning Tools and Techniques*. en. Elsevier, 2011. ISBN: 978-0-12-374856-0. DOI: 10.1016/C2009-0-19715-5. URL: <https://linkinghub.elsevier.com/retrieve/pii/C20090197155> (visited on 07/14/2020).
- [35] Christopher M. Bishop. *Pattern recognition and machine learning*. en. Information science and statistics. New York: Springer, 2006. ISBN: 978-0-387-31073-2.